

Research Article

Dynamical Analysis of the Global Warming

J. A. Tenreiro Machado¹ and António M. Lopes²

¹ *Department of Electrical Engineering, Institute of Engineering of Porto,
Rua Dr. António Bernardino de Almeida 431, 4200-072 Porto, Portugal*

² *IDMEC-Pólo FEUP, Faculdade de Engenharia, Universidade do Porto,
Rua Dr. Roberto Frias, 4200-465 Porto, Portugal*

Correspondence should be addressed to J. A. Tenreiro Machado, jtm@isep.ipp.pt

Received 17 September 2012; Accepted 31 October 2012

Academic Editor: Clara Lonescu

Copyright © 2012 J. A. Tenreiro Machado and A. M. Lopes. This is an open access article distributed under the Creative Commons Attribution License, which permits unrestricted use, distribution, and reproduction in any medium, provided the original work is properly cited.

Global warming is a major concern nowadays. Weather conditions are changing, and it seems that human activity is one of the main causes. In fact, since the beginning of the industrial revolution, the burning of fossil fuels has increased the nonnatural emissions of carbon dioxide to the atmosphere. Carbon dioxide is a greenhouse gas that absorbs the infrared radiation produced by the reflection of the sunlight on the Earth's surface, trapping the heat in the atmosphere. Global warming and the associated climate changes are being the subject of intensive research due to their major impact on social, economic, and health aspects of human life. This paper studies the global warming trend in the perspective of dynamical systems and fractional calculus, which is a new standpoint in this context. Worldwide distributed meteorological stations and temperature records for the last 100 years are analysed. It is shown that the application of Fourier transforms and power law trend lines leads to an assertive representation of the global warming dynamics and a simpler analysis of its characteristics.

1. Introduction

The standard approach for modelling natural and artificial phenomena in the perspective of dynamical systems is to adopt the tools of mathematics and, in particular, the classical integral and differential calculus.

Fractional calculus (FC) is a common expression that is used to denote the branch of calculus that extends the concepts of integrals and derivatives to noninteger and complex orders [1–9]. During the last decade FC was found to play a fundamental role in the modelling of a considerable number of phenomena [10–15] and emerged as an important tool for the study of dynamical systems where classical methods reveal strong limitations. As a consequence, nowadays, the application of FC concepts encompasses a wide spectrum

of studies [16–19], ranging from dynamics of financial markets [20, 21], biological systems, [22, 23] and DNA sequencing [24] up to mechanical [13, 25–28] and electrical systems [29–31].

The generalization of the concept of derivative and integral to noninteger orders, α , has been addressed by many mathematicians. The Riemann-Liouville, Grünwald-Letnikov, and Caputo definitions of fractional derivative, given by (1.1)–(1.3), are the most used [32]:

$${}^{\text{RL}}D_t^\alpha f(t) = \frac{1}{\Gamma(n-\alpha)} \frac{d^n}{dt^n} \int_a^t \frac{f(\tau)}{(t-\tau)^{\alpha-n+1}} d\tau, \quad n-1 < \alpha < n, \quad (1.1)$$

$${}^{\text{GL}}D_t^\alpha f(t) = \lim_{h \rightarrow 0} \frac{1}{h^\alpha} \sum_{k=0}^{[(t-a)/h]} (-1)^k \binom{\alpha}{k} f(t-kh), \quad (1.2)$$

$${}^{\text{C}}D_t^\alpha f(t) = \frac{1}{\Gamma(n-\alpha)} \int_a^t \frac{f^{(n)}(\tau)}{(t-\tau)^{\alpha-n+1}} d\tau, \quad n-1 < \alpha < n, \quad (1.3)$$

where $\Gamma(\cdot)$ represents the Euler's gamma function, the operator $[x]$ is the integer part of x , and h is a time step.

The Laplace transform applied to (1.1) yields

$$L\left\{{}^{\text{RL}}D_t^\alpha f(t)\right\} = s^\alpha L\{f(t)\} - \sum_{k=0}^{n-1} s^k {}^{\text{RL}}D_t^{\alpha-k-1} f(0^+), \quad (1.4)$$

where L and s denote the Laplace operator and variable, respectively.

The Mittag-Leffler (M-L) function, $E_\alpha(t)$, plays an important role in the context of FC, being defined by

$$E_\alpha(t) = \sum_{k=0}^{\infty} \frac{t^k}{\Gamma(\alpha k + 1)}. \quad (1.5)$$

This function establishes a connection between purely exponential and power law behaviours that characterize integer and fractional order phenomena, respectively. In particular, if $\alpha = 1$, then $E_1(t) = e^t$. For large values of t , $E_\alpha(t)$ has the asymptotic behaviour:

$$E_\alpha(-t) \approx \frac{1}{\Gamma(1-\alpha)} \frac{1}{t}, \quad \alpha \neq 1, \quad 0 < \alpha < 2. \quad (1.6)$$

The Laplace transform (1.7) permits a natural extension of transform pairs from exponential function and integer powers of s towards M-L function and fractional powers of s :

$$L\{E_\alpha(-at^\alpha)\} = \frac{s^{\alpha-1}}{s^\alpha + a}. \quad (1.7)$$

The generalization promoted by FC leads directly to fractional dynamical models, but the fact is that neither their limits of application nor the methods and tools for capturing them seem to be well defined at the present stage of scientific knowledge.

This paper studies the complex dynamics characteristics of the global warming. It is believed that human activity is the main cause of such a phenomenon, and dramatic consequences to the planet are expected if the warming trend observed in the last century persists. The main goal is to analyse and discuss the characteristics of the global warming in the perspective of dynamical systems, which is a new standpoint in this context. It is shown that the application of Fourier transforms and power law trend lines leads to an assertive representation of the global warming dynamics and a simpler analysis of its characteristics.

The paper is organized as follows. Section 2 contextualizes the main subject. A heuristic approach to analyse the data from the meteorological stations in the time domain is proposed, and several characteristics of the global warming are exposed. Section 3 formulates the framework of the analysis in the perspective of FC and analyses the fractional dynamics of the system. Finally, Section 4 outlines the main conclusions.

2. Characteristics of the Global Warming

Earth is warming, and it seems that human activity and solar effects are the main probable causes [33–35]. Some impacts such as the record of high temperatures, the melting glaciers, and severe flooding are becoming increasingly common across the countries and around the world [36, 37]. Aside from the effect on temperature, warming leads to the modification of wind patterns, the development of humidity, and the alteration of the rates of precipitation. These phenomena are being the subject of intensive research due to major impact on social, economic, and health aspects of human life [38–40].

Figures 1 and 2 show average temperatures computed for two decades separated by almost one hundred years. The white marks on the maps represent meteorological stations. Figure 1 is the contour plot of the worldwide temperatures corresponding to the period 1910–1919, and Figure 2 corresponds to the period 2000–2009. The temperature difference between the two decades is presented in Figure 3, showing that the northern hemisphere has been more affected by warming.

In our study, the Global Historical Climatology Network-Monthly (GHCN-M), version 3 dataset of monthly mean temperature [41], available at the National Oceanic and Atmospheric Administration, National Climatic Data Center (NOAA-NCDC) (<http://www.ncdc.noaa.gov/ghcnm/v3.php>), is used. The current archive contains temperature records from 7280 meteorological stations located on land areas. However, few stations have long records, and these are essentially restricted to the northern hemisphere (the United States and Western Europe). As the computation of the Fourier transform requires quite long time series, a sample of 210 worldwide meteorological stations, distributed as uniformly as possible, and having 100 years length records, was selected. Most stations of Africa, Alaska, Canada and the northern and southern regions of the globe do not meet the previous condition, which means that the results for these regions (and also for sea areas), plotted on the maps, may be less accurate.

Each data record consists of the average temperatures per month. Some occasional gaps of one month in the data (represented on the original data by the value -9999) are substituted by a linear interpolation between the two adjacent values. Moreover, although of minor influence, the distinct number of days of each month and the leap years are also taken into account. For the whole sample of meteorological stations, as the data is available for slightly different periods of time, depending on the station, the period from January 1910 up to December 2010 is considered for all cases.

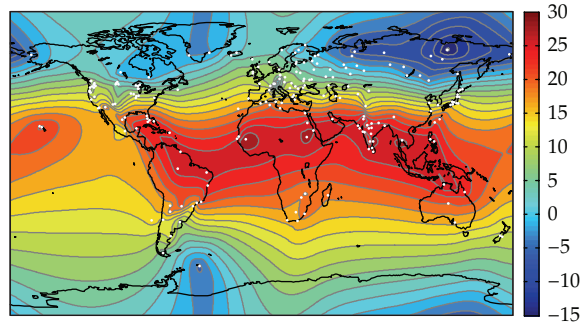


Figure 1: Global average temperatures: decade 1910–1919.

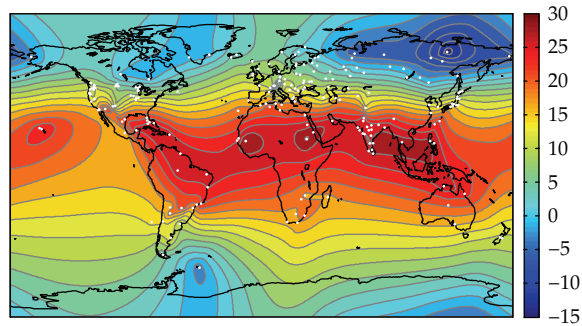


Figure 2: Global average temperatures: decade 2000–2009.

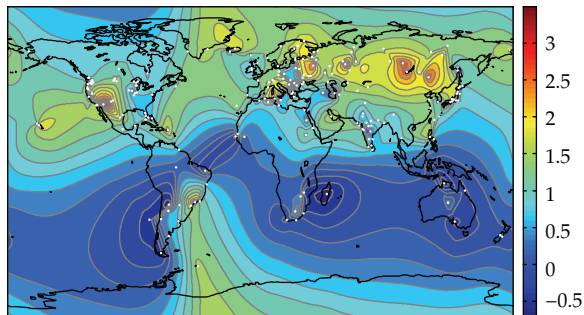


Figure 3: Temperature difference between decades 2000–2009 and 1910–1919.

Figure 4 depicts the time evolution of the monthly average temperature of one typical station (Tokyo, Japan, Lat 35.67 N, Lon 139.75 W), where three processes are visible, namely, (i) a continuous, almost linear, temperature increase, (ii) an annual periodic variation, and (iii) a “random” temperature variation that may be the symptom of a fractional dynamical behaviour.

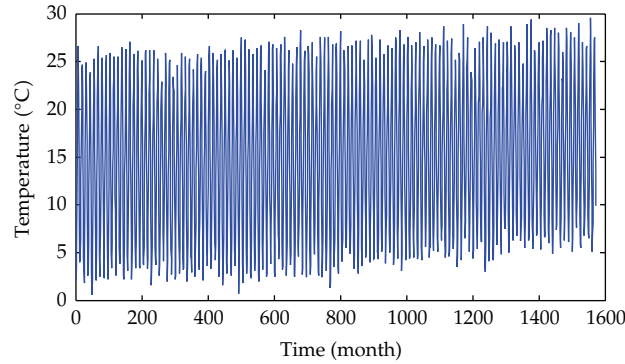


Figure 4: Monthly average temperatures for Tokyo, Japan, meteorological station (January 1881–August 2011).

In this study, a heuristic decomposition of the time series is first proposed. The temperature signal from the i th meteorological station, $T_i(t)$, $i = 1, \dots, 210$, is approximated by the sum given in the following:

$$T_i(t) \approx a_0 + a_1 \cdot t + a_2 \cdot \sin(\omega \cdot t + a_3) + a_4 \cdot \sin(2\omega \cdot t + a_5), \quad (2.1)$$

where t is time, $\omega = 2\pi/T$ represents the angular frequency, and T is one year.

The coefficients a_0 and a_1 are the parameters of a trend line adjusted to the original data, $T_i(t)$, using the least squares algorithm. This trend line is then subtracted from the signal $T_i(t)$, and, for the result, the two first harmonics of the Fourier series are calculated. The corresponding coefficients are (a_2, a_3) and (a_4, a_5) , respectively.

Figures 5–11 show the mapping of the coefficients. Coefficient a_0 is closely related to the average temperature and highlights the warmer regions of the globe (Figure 5), whereas coefficient a_1 (Figure 6) emphasizes the gradient of temperature increase. Consequently, Figure 6 is highly correlated with Figure 3.

The parameters of the first harmonic, namely, a_2 and a_3 , are depicted in Figures 7 and 8, respectively. The amplitude of the sinusoid (Figure 7) unveils a strong mark centred in Siberia and a weaker, but also clear, mark in North America, respectively. Figure 8 represents the map of coefficient a_3 , corresponding to the phase of the sine function. As expected, northern and southern hemispheres are in phase opposition. The analysis and physical meaning of the coefficients a_4 and a_5 that correspond to the second harmonic of the heuristic approximation are more difficult and seem to point to a less significant meaning (Figures 9 and 10). Nevertheless, those parameters might also reveal relationships hidden in the data that can trigger a future comprehensive explanation of these phenomena.

It is important to notice that the heuristic approximation given by (2.1) captures most of the energy of the original signals. Moreover, the energy contained in the second harmonic is almost negligible. This is illustrated in Figures 11 and 12. Figure 11 represents the percentage of energy captured by the heuristic approximation with reference to the total energy of the original signals, revealing a percentage in the interval [86% 99%]. Figure 12 represents the case of not including the second harmonic. We verify that it exhibits only slight differences when compared to the previous one.

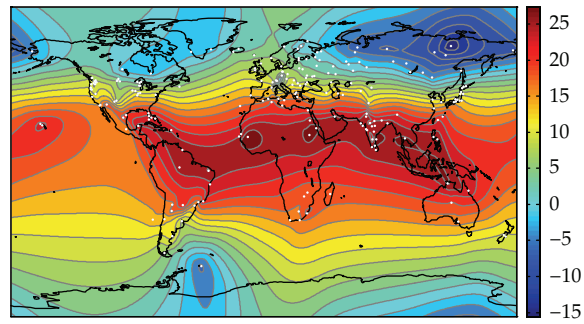


Figure 5: Map of coefficient a_0 of expression (2.1).

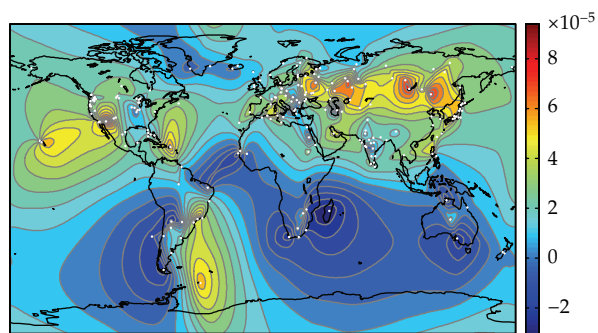


Figure 6: Map of coefficient a_1 of expression (2.1).

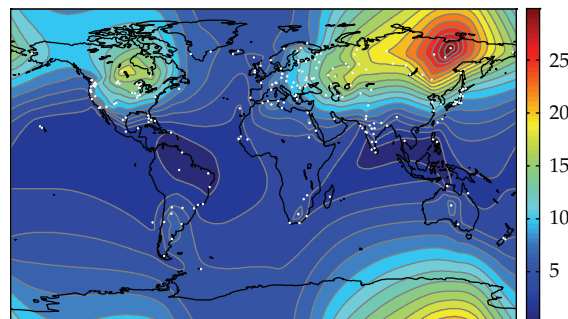


Figure 7: Map of coefficient a_2 of expression (2.1).

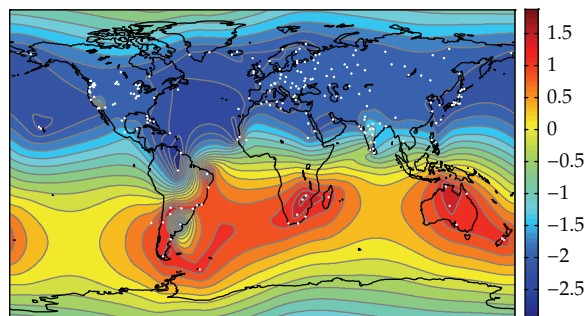


Figure 8: Map of coefficient a_3 of expression (2.1).

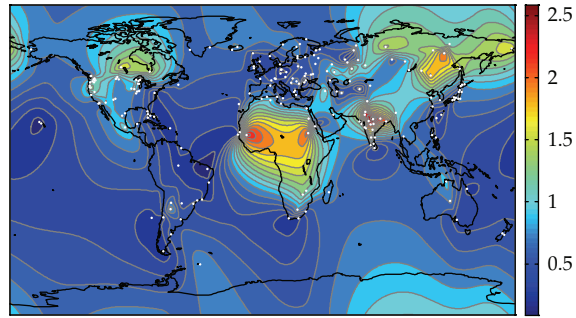


Figure 9: Map of coefficient a_4 of expression (2.1).

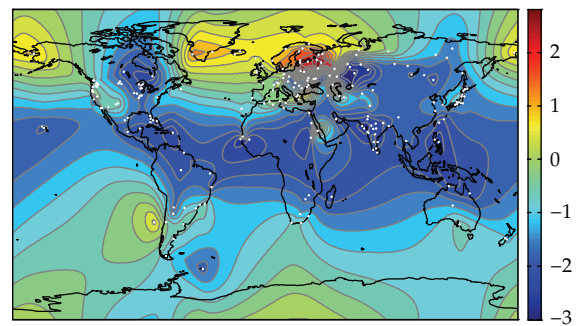


Figure 10: Map of coefficient a_5 of expression (2.1).

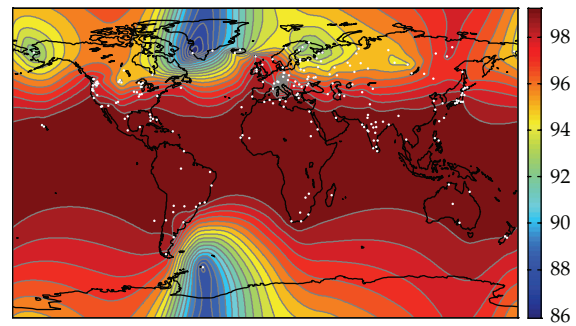


Figure 11: Percentage of energy of the heuristic approximation with reference to the total energy of the original signals.

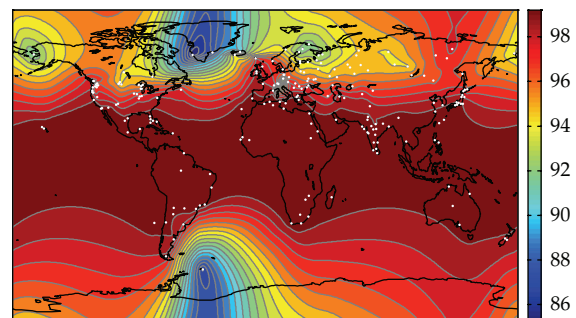


Figure 12: Percentage of energy of the heuristic approximation (without second harmonic) with reference to the total energy of the original signals.

3. Dynamics of the Global Warming

In this section, the global warming phenomenon is analysed in the perspective of a complex system that reacts to stimuli, being the response signals studied by means of the Fourier transform. The methodology is to obtain a representative signal as a manifestation of the system dynamics, process it with the Fourier transform, and, given the characteristics of the resulting spectrum, to approximate its amplitude by means of a power function.

In analytical terms, for a continuous signal $x(t)$, evolving in the time domain t , we have

$$F\{x(t)\} = X(j\omega) = \int_{-\infty}^{+\infty} x(t) \cdot e^{-j\omega t} \cdot dt, \quad (3.1)$$

where F represents the Fourier operator, ω is the angular frequency, and $j = \sqrt{-1}$.

The power law approximation is given by

$$|F\{x(t)\}| = |X(j\omega)| = a \cdot \omega^b, \quad a \in \mathfrak{R}^+, b \in \mathfrak{R}. \quad (3.2)$$

The parameters of the power law are the pair (a, b) to be determined by the least squares fit procedure.

Figure 13 depicts the amplitude of the Fourier transform obtained for the meteorological station Tokyo (Figure 4), where a peak value at the angular frequency $\omega = 1.99 \times 10^{-7}$ rad/s that corresponds to a periodicity of one year is well visible.

At low frequencies (Figure 14), it is clear that the spectrum can be approximated by a power law with parameters $(a, b) = (292.1047, -0.8397)$, leading to a fractional value of parameter b .

In the sequel, the values of (a, b) were computed for the whole sample of meteorological stations, using the least squares fit procedure. It was found that there exists a strong correlation between the two parameters. In fact, Figure 15 illustrates clearly the relation between $\log(a)$ and b . It can be seen that a straight line fits quite well into the data. Figures 16 and 17 depict the contour plots of $\log(a)$ and b , respectively. Therefore, we will concentrate our attention on one parameter only, namely, on b that represents the variation of the signal energy versus ω .

The map of parameter b (Figure 17) reveals that climate changes are taking place in the northern hemisphere. Two large regions of Russia and Canada and, in a less extent, central Europe and Western Alaska are being the most affected areas.

As expected, Figure 16 is somewhat "redundant," since Figure 17, with parameter b , is sufficient to characterize the warming dynamics. We verify that $\text{abs}(b)$ varies between 0 and 1 that can be viewed as the cases of white and pink noises, respectively. Therefore, we conclude that equatorial and south hemisphere regions exhibit more "correlated" variation, while the north hemisphere and the two poles have a more "erratic" variation of the temperature.

These results are of utmost importance because we can capture and analyse all information through a single map. In a different perspective, we should also note that the adoption of FC concepts captures large memory effects present in long time series, which is the case of Earth's warming. Therefore, these results encourage further research in this line of thought.

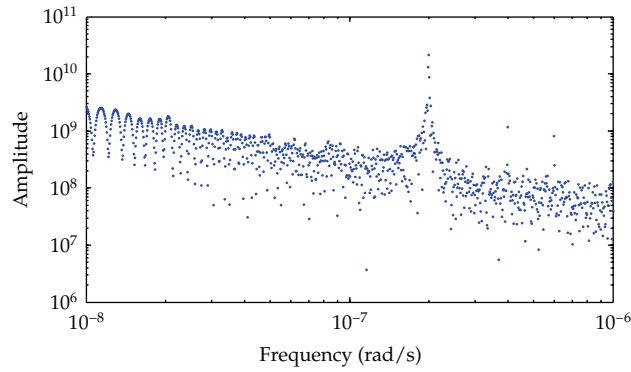


Figure 13: Amplitude of the Fourier transform of the monthly average temperatures of Tokyo.

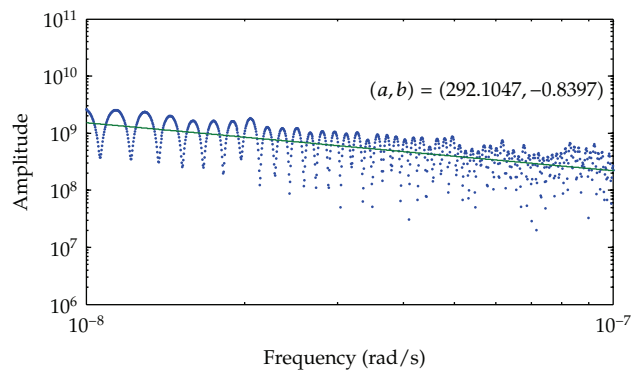


Figure 14: Power law approximation of the amplitude of the Fourier transform of the monthly average temperatures of Tokyo.

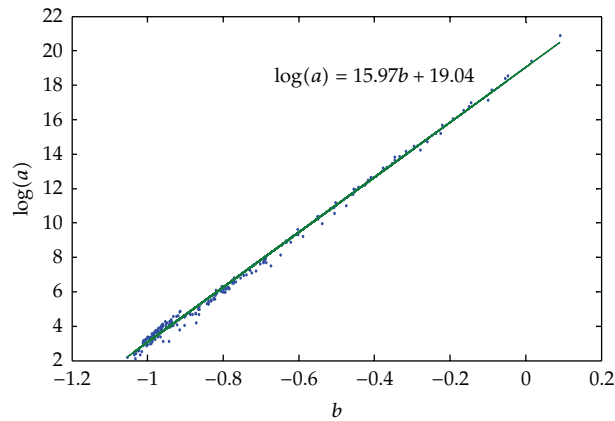


Figure 15: Mapping of the power law parameters $[\log(a), b]$.

4. Conclusions

This paper analysed the global warming in the perspective of complex systems dynamics. The use of Fourier transforms and power law trend lines revealed fractional order dynamics characteristics of the phenomenon. While classical mathematical tools could be adopted,

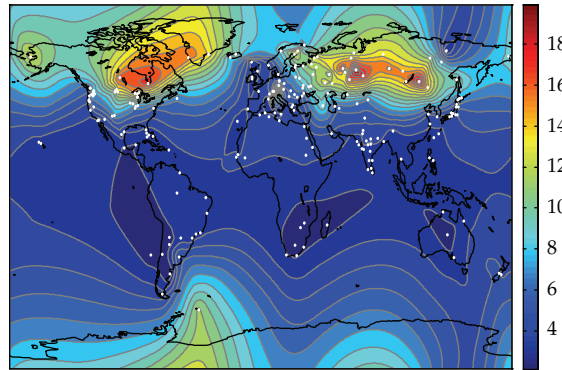


Figure 16: Contour plot of parameter $\log(a)$.

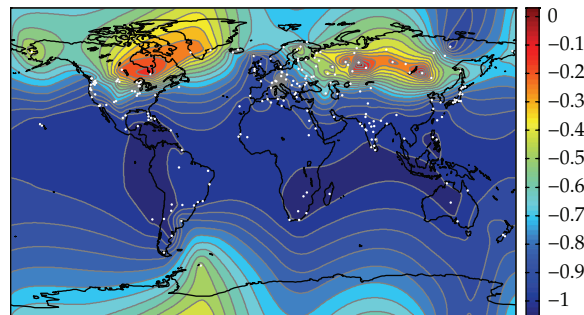


Figure 17: Contour plot of parameter b .

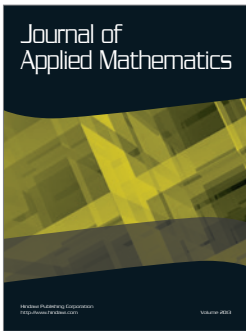
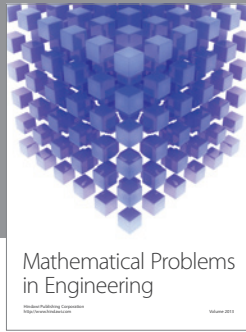
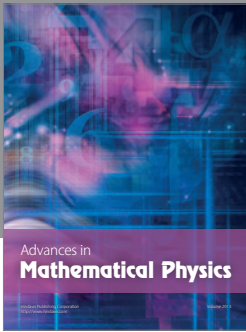
the used methodology based on FC concepts leads to simpler and assertive representation of the global warming dynamics. FC captures inherently long range effects that are overlooked by classical methods. Therefore, this study motivates the analysis of global phenomena with long time histories bearing in mind FC.

References

- [1] S. G. Samko, A. A. Kilbas, and O. I. Marichev, *Fractional Integrals and Derivatives: Theory and Applications*, Gordon and Breach Science Publishers, London, UK, 1993.
- [2] K. S. Miller and B. Ross, *An Introduction to the Fractional Calculus and Fractional Differential Equations*, John Wiley & Sons, New York, NY, USA, 1993.
- [3] I. Podlubny, *Fractional Differential Equations: An Introduction to Fractional Derivatives, Fractional Differential Equations, to Methods of Their Solution and Some of Their Applications*, vol. 198 of *Mathematics in Science and Engineering*, Academic Press, San Diego, Calif, USA, 1999.
- [4] A. A. Kilbas, H. M. Srivastava, and J. J. Trujillo, *Theory and Applications of Fractional Differential Equations*, vol. 204 of *North-Holland Mathematics Studies*, Elsevier Science B.V., Amsterdam, The Netherlands, 2006.
- [5] K. Diethelm, *The Analysis of Fractional Differential Equations: An Application-Oriented Exposition using Differential Operators of Caputo Type*, vol. 2004 of *Lecture Notes in Mathematics*, Springer, Berlin, Germany, 2010.
- [6] D. Baleanu, K. Diethelm, E. Scalas, and J. J. Trujillo, *Fractional Calculus: Models and Numerical Methods*, vol. 3 of *Series on Complexity, Nonlinearity and Chaos*, World Scientific Publishing, Singapore, 2012.
- [7] M. D. Ortigueira, *Fractional Calculus for Scientists and Engineers*, vol. 84 of *Lecture Notes in Electrical Engineering*, Springer, Dordrecht, The Netherlands, 2011.

- [8] R. R. Nigmatullin, I. I. Popov, and D. Baleanu, "Predictions based on the cumulative curves: basic principles and nontrivial example," *Communications in Nonlinear Science and Numerical Simulation*, vol. 16, no. 2, pp. 895–915, 2011.
- [9] D. Baleanu and J. I. Trujillo, "A new method of finding the fractional Euler-Lagrange and Hamilton equations within Caputo fractional derivatives," *Communications in Nonlinear Science and Numerical Simulation*, vol. 15, no. 5, pp. 1111–1115, 2010.
- [10] A. Oustaloup, *La Commande CRONE: Commande Robuste d'Ordre Non Entier*, Hermès, Paris, France, 1991.
- [11] G. M. Zaslavsky, *Hamiltonian Chaos and Fractional Dynamics*, Oxford University Press, Oxford, UK, 2008.
- [12] R. Magin, *Fractional Calculus in Bioengineering*, Begell House Publishers, Redding, Calif, USA, 2006.
- [13] F. Mainardi, *Fractional Calculus and Waves in Linear Viscoelasticity: An Introduction to Mathematical Models*, Imperial College Press, London, UK, 2010.
- [14] C. Monje, Y. Chen, B. Vinagre, D. Xue, and V. Feliu, *Fractional Order Systems and Controls: Fundamentals and Applications*, Springer, London, UK, 2010.
- [15] J. T. Machado, V. Kiryakova, and F. Mainardi, "Recent history of fractional calculus," *Communications in Nonlinear Science and Numerical Simulation*, vol. 16, no. 3, pp. 1140–1153, 2011.
- [16] T. Anastasio, "The fractional-order dynamics of brainstem vestibulooculomotor neurons," *Biological Cybernetics*, vol. 72, pp. 69–79, 1994.
- [17] J.-G. Lu and Y.-Q. Chen, "Robust stability and stabilization of fractional-order interval systems with the fractional order α : the $0 < \alpha < 1$ case," *Institute of Electrical and Electronics Engineers*, vol. 55, no. 1, pp. 152–158, 2010.
- [18] D. Baleanu, A. K. Golmankhaneh, A. K. Golmankhaneh, and R. R. Nigmatullin, "Newtonian law with memory," *Nonlinear Dynamics*, vol. 60, no. 1-2, pp. 81–86, 2010.
- [19] C. M. Ionescu, J. A. T. Machado, and R. De Keyser, "Modeling of the lung impedance using a fractional-order ladder network with constant phase elements," *IEEE Transactions on Biomedical Circuits and Systems*, vol. 5, no. 1, pp. 83–89, 2011.
- [20] E. Scalas, R. Gorenflo, and F. Mainardi, "Fractional calculus and continuous-time finance," *Physica A*, vol. 284, no. 1–4, pp. 376–384, 2000.
- [21] F. B. Duarte, J. A. Tenreiro Machado, and G. M. Duarte, "Dynamics of the Dow Jones and the NASDAQ stock indexes," *Nonlinear Dynamics*, vol. 61, no. 4, pp. 691–705, 2010.
- [22] C. M. Ionescu, P. Segers, and R. De Keyser, "Mechanical properties of the respiratory system derived from morphologic insight," *IEEE Transactions on Biomedical Engineering*, vol. 56, no. 4, pp. 949–959, 2009.
- [23] C. Ionescu and J. T. MacHado, "Mechanical properties and impedance model for the branching network of the sapping system in the leaf of *Hydrangea Macrophylla*," *Nonlinear Dynamics*, vol. 60, no. 1-2, pp. 207–216, 2010.
- [24] J. A. Tenreiro Machado, A. C. Costa, and M. D. Quelhas, "Fractional dynamics in DNA," *Communications in Nonlinear Science and Numerical Simulation*, vol. 16, no. 8, pp. 2963–2969, 2011.
- [25] W. H. Deng and C. P. Li, "Chaos synchronization of the fractional Lü system," *Physica A*, vol. 353, no. 1–4, pp. 61–72, 2005.
- [26] R. R. Nigmatullin, "Fractional kinetic equations and universal decoupling of a memory function in mesoscale region," *Physica A*, vol. 363, no. 2, pp. 282–298, 2006.
- [27] O. P. Agrawal, "Fractional variational calculus in terms of Riesz fractional derivatives," *Journal of Physics A*, vol. 40, no. 24, pp. 6287–6303, 2007.
- [28] A. Oustaloup, X. Moreau, and M. Nouillant, "The crone suspension," *Control Engineering Practice*, vol. 4, no. 8, pp. 1101–1108, 1996.
- [29] A. G. Radwan, A. M. Soliman, and A. S. Elwakil, "Design equations for fractional-order sinusoidal oscillators: four practical circuit examples," *International Journal of Circuit Theory and Applications*, vol. 36, no. 4, pp. 473–492, 2008.
- [30] I. Petráš, "A note on the fractional-order Chua's system," *Chaos, Solitons and Fractals*, vol. 38, no. 1, pp. 140–147, 2008.
- [31] H. Cao, Z. Deng, X. Li, J. Yang, and Y. Qin, "Dynamic modeling of electrical characteristics of solid oxide fuel cells using fractional derivatives," *International Journal of Hydrogen Energy*, vol. 35, no. 4, pp. 1749–1758, 2010.
- [32] J. A. Tenreiro Machado, "Fractional order modelling of fractional-order holds," *Nonlinear Dynamics*, vol. 70, pp. 789–796, 2012.

- [33] M. R. Allen, D. J. Frame, C. Huntingford et al., "Warming caused by cumulative carbon emissions towards the trillionth tonne," *Nature*, vol. 458, no. 7242, pp. 1163–1166, 2009.
- [34] A. Dai, "Drought under global warming: a review," *WIREs Climate Change*, vol. 2, no. 1, pp. 45–65, 2011.
- [35] Q. You, S. Kang, N. Pepin et al., "Climate warming and associated changes in atmospheric circulation in the eastern and central Tibetan Plateau from a homogenized dataset," *Global and Planetary Change*, vol. 72, no. 1–2, pp. 11–24, 2010.
- [36] S. Jevrejeva, J. C. Moore, and A. Grinsted, "Sea level projections to AD2500 with a new generation of climate change scenarios," *Global and Planetary Change*, vol. 80-81, pp. 14–20, 2012.
- [37] C. Giannakopoulos, P. Le Sager, M. Bindi, M. Moriondo, E. Kostopoulou, and C. M. Goodess, "Climatic changes and associated impacts in the Mediterranean resulting from a 2 °C global warming," *Global and Planetary Change*, vol. 68, no. 3, pp. 209–224, 2009.
- [38] J. Hansen, R. Ruedy, M. Sato, and K. Lo, "Global surface temperature change," *Reviews of Geophysics*, vol. 48, Article ID RG4004, 2010.
- [39] P. Brohan, J. J. Kennedy, I. Harris, S. F. B. Tett, and P. D. Jones, "Uncertainty estimates in regional and global observed temperature changes: a new data set from 1850," *Journal of Geophysical Research D*, vol. 111, no. 12, Article ID D12106, 2006.
- [40] M. J. Menne and C. N. Williams, "Homogenization of temperature series via pairwise comparisons," *Journal of Climate*, vol. 22, no. 7, pp. 1700–1717, 2009.
- [41] J. H. Lawrimore, M. J. Menne, B. E. Gleason et al., "An overview of the Global Historical Climatology Network monthly mean temperature data set, version 3," *Journal of Geophysical Research*, vol. 116, Article ID D19121, 18 pages, 2011.




Hindawi

Submit your manuscripts at
<http://www.hindawi.com>

